JOURNAL OF CATALYSIS 131, 1–21 (1991)

CO Oxidation over Pd and Cu Catalysts

III. Reduced Al_2O_3-Supported Pd

KYUNG I. CHOI AND M. ALBERT VANNICE[1]

Department of Chemical Engineering, The Pennsylvania State University, University Park, Pennsylvania 16802

Received November 14, 1990; revised April 19, 1991

CO oxidation by O_2 over Pd was studied between 300 and 450 K and at relatively high partial pressures (up to 100 Torr CO and 180 Torr O_2). As the temperature increased, the apparent activation energy increased, the pressure dependency on CO changed from near 0 to -1, and above 50 Torr the O_2 dependency increased from 0.2 to 0.7. Below 400 K a first-order O_2 dependence was observed at lower O_2 pressures. IR spectra were obtained under steady-state reaction conditions to monitor the CO species present on the Pd surface. The spectra were consistent with the negative-order dependence on CO and higher rates were observed when the surface concentration of CO decreased, and they also provided evidence for compressed layers of CO below 400 K. At the higher O_2 pressures employed, a normal Langmuir–Hinshelwood (L–H) model appears applicable in the regime above 400 K, whereas a reaction between CO and O atoms at the perimeters of their respective islands seems more appropriate below 400 K. The rate parameters derived from the two rate equations are extremely consistent with this transformation as the activation energy of the rate-determining step shifted from 15 kcal/mole in the island regime to 23 kcal/mole in the normal L–H regime, in agreement with the shift from 14 to 25 kcal/mole reported by Engel and Ertl on a Pd(111) surface. Furthermore, the heats of adsorption derived from the K_{CO} and K_{O_2} values in the L–H rate expression are similar to Q_{ad} values reported on nearly saturated Pd surfaces, while the values obtained from the island rate expression are lower, which is expected if compression occurs. Under conditions where O_2 adsorption appeared to be the slow step, this elementary step appeared to remain nonactivated.

INTRODUCTION

The CO oxidation reaction is important because of the need to remove CO from the exhaust gas stream of both mobile and stationary power sources. This reaction over Group VIII metals was first studied by Langmuir in 1922 (*1*), and it still remains worthy of investigation because of certain characteristics it possesses. Even though the overall reaction looks very simple, namely,

$$2\ CO + O_2 \rightarrow 2\ CO_2, \qquad (1)$$

the reaction kinetics are in fact rather complicated, and various phenomena have been associated with its occurrence on Pd, such as: rate dependencies varying from negative first order to positive first order for each reactant (*2–7*), surface diffusion of adsorbed CO (*2, 8–11*), adsorbate island formation (*3, 12–14*), stable rate oscillations (*15–17*), and metal surface restructuring under reaction conditions (*18*). The interpretation of these results has been complicated, but these and other studies have provided a much better understanding of the surface chemistry associated with this reaction.

This reaction has been studied frequently over both single-crystal Pd surfaces and supported Pd crystallites, and the evidence overwhelmingly favors a model involving a surface reaction between an adsorbed CO molecule and an oxygen atom. However, different rate expressions have been reported in different reaction regimes. For example, at high surface coverages of CO and lower tem-

[1] To whom correspondence should be addressed.

0021-9517/91 $3.00

peratures, the dissociative adsorption of oxygen molecules can be inhibited when O_2 pressures are low, and this gives a first-order O_2 dependence and a negative reaction-order dependency on the CO concentration (*2*). In contrast, at higher temperatures and higher O_2/CO ratios, these dependencies are reversed (*7*), and domains of adsorbed oxygen atoms can form creating compressed adsorbed CO species (*2*). Under these conditions, the reaction is presumed to occur only around the perimeter of these islands, and a recent study has shown that a model invoking islands can describe the data well (*14*). Despite the number of studies pertaining to this reaction, only two infrared investigations under steady-state reaction conditions have been reported (*19, 20*). However, both were conducted under low CO and O_2 pressures and neither determined the rate expression appropriate for the reaction conditions employed although Baddour *et al.* examined the effect of partial pressures and calculated an apparent activation energy (*19*).

This investigation was part of a program to investigate the reaction between CO and O_2 over prereduced Pd/δ-Al_2O_3, Cu/δ-Al_2O_3, and bimetallic Pd-Cu/δ-Al_2O_3 catalysts and to compare their behavior with the unreduced $PdCl_2$, $CuCl_2$, and mixed $PdCl_2$–$CuCl_2$ salts on δ-Al_2O_3, which can be extremely active catalysts (*21, 22*). An *in situ* IR/reactor system was utilized to simultaneously determine reaction kinetics and obtain IR spectra under differential, steady-state conditions. In addition, much higher partial pressures of each reactant were used so that the regime including the use of air as the oxygen source was encompassed, and relatively low temperatures (300–450 K) were also employed. This combination represents a reaction regime that has been infrequently studied. This paper describes CO oxidation over Pd/δ-Al_2O_3 catalysts, while the other two catalyst systems are discussed subsequently (*23, 24*).

EXPERIMENTAL

The supported Pd catalysts were made by an incipient wetness method (*25*). The δ-Al_2O_3 support and metal precursor are identical to those used to prepare the Pd-only catalyst described previously (*21*), i.e., δ-Al_2O_3 (W. R. Grace, 138 m^2/g) and $PdCl_2$ (Alfa Products), respectively, and the η-Al_2O_3 support has been described previously (*25*). Before preparing these catalysts, the Al_2O_3 was ground and sieved to a 40/80 mesh size and calcined in dry air (825 cm^3/min) at 723 K for 2.5 h. Catalyst preparation was based upon established methods (*25–27*), and after impregnation of the Al_2O_3 with the $PdCl_2$ solution, the catalyst was dried overnight in an oven at 393 K and again calcined at 673 K in dry air (825 cm^3/min) for 2 h.

The reduction procedure in the reactor or the adsorption system was as follows: the catalyst was exposed to flowing He (30 cm^3/min) at 300 K, then the temperature was increased to 573 K and held there for 1 h. The He flow was switched to H_2 (30 cm^3/min) and the catalyst was reduced at 573 K for 1 h and then purged with flowing He (30 ml/min) for 1 h at the same temperature before it was cooled to 300 K. Standard chemisorption methods using H_2, O_2, and CO were employed to measure the number of surface Pd atoms (*26, 27*) and to allow calculation of a turnover frequency (TOF). Sample preparation, equipment, and data acquisition methods are the same as those described earlier (*21*). Kinetic data were obtained in a stainless-steel microreactor using powdered catalysts as well as in the IR reactor system to ensure that the results from the pressed disc of catalyst in the IR reactor were reproducible. The Pd loadings were determined by plasma emission spectroscopy on the fresh sample after drying at 393 K.

RESULTS

Chemisorption of H_2, CO, and O_2 was measured on both fresh, reduced catalyst samples and on used samples after the kinetic runs. These uptakes, the calculated Pd dispersions (fractions exposed) assuming $H_{ad}/Pd_s = 1$ and $CO_{ad}/Pd_s = 1$, and the apparent bulk hydride ratios are listed in Table 1. Here Pd_s represents a surface atom.

TABLE 1

Characterization of Pd/Al_2O_3 Catalysts by Chemisorption

Catalyst	Irreversible uptake (μmole/g cat)			Disp.[a] (%)	Particle size (Å)	Hydride ratio (H/Pd_{bulk})
	H_2	O_2	CO[b]			
2.33% Pd/η-Al_2O_3 (Fresh)	59.7	—	—	55	21	0.61
2.33% Pd/η-Al_2O_3 (Reactor)	32.5	—	61.3	30	38	0.47
2.10% Pd/δ-Al_2O_3 (Fresh)	49.3	—	83.3	50	23	0.55
	40.0	—	83.5	41	28	0.52
	39.5	—	80.0	40	28	0.52
2.10% Pd/δ-Al_2O_3 (Reactor)	16	—	33.5	16	69	0.52
2.10% Pd/δ-Al_2O_3 (IR)	3.0	19.5	38.7	39[c]	29	0.45
	4.5	—	—			0.41
	12.0[d]	—	—			0.48
2.19% Pd/δ-Al_2O_3 (Fresh)	53.3	—	—	52	22	0.67
	50.0	32.8	—	49	23	0.62
	55.0	35.0	98.0	53	21	0.63
2.19% Pd/δ-Al_2O_3	31.0	20.0	60.0	30	37	0.51
2.19% Pd/δ-Al_2O_3 (IR)	11.5	—	—	11	101	0.40
	17.1	16.7	36.3	17	68	0.40
	17.0	—	—	17	68	0.40

[a] Calculated from H_2 uptake assuming $H_{ad}/Pd_s = 1$.
[b] Total uptake (reversible uptake is not subtracted because no uptake was observed with pure δ-Al_2O_3.
[c] Calculated from CO uptake.
[d] Obtained after 383 K O_2 treatment for 1 h.

A summary of the kinetic behavior of the prereduced Pd/Al_2O_3 catalysts is given in Tables 2 and 3, and typical Arrhenius plots for these catalysts are shown in Figs. 1 and 2. Specific activities are reported in the form of a turnover frequency (TOF = molecule $\cdot$ s^{-1} $\cdot$ Pd_s^{-1}), based on H chemisorption on the used samples, as listed in Table 1. Partial pressure dependencies were determined over certain pressure regimes, which were from 0.5 to 26 Torr for CO and from 26 to 184 Torr for O_2. The runs conducted in the microreactor are shown in Figs. 3 and 4 along with the power rate law providing the best fit in various pressure ranges.

The apparent activation energies, E_{app}, for the Al_2O_3-supported Pd catalysts are also listed in Table 2. With the 2.10% Pd/δ-Al_2O_3 below 400 K, an activation energy of 11.0 kcal/mole was obtained in the microreactor and a value of 10.6 kcal/mole was measured in the IR reactor. With the 2.19% Pd/δ-Al_2O_3 in the same microreactor system, another kinetic study was performed and an activation energy of 9.7 kcal/mole was measured below 400 K, which was similar to that for the first 2.10% Pd/δ-Al_2O_3 catalyst, while two runs in the IR reactor gave values of 12.4 and 11.6 kcal/mole. These initial kinetic studies were conducted in a relatively low temperature region (below 413 K); however, a trend to higher E_{app} values as the temperature increased was apparent, so the last kinetic run in Table 2 was obtained in a higher temperature region (between 393 and 453 K). It was conducted with a $\left(\frac{3}{16}\right)$-in. stainless-steel microreactor tube instead of a $\left(\frac{1}{4}\right)$-in. tube because a much smaller amount of catalyst had to be used to prevent the conversion of CO to CO_2 from being too high in this higher temperature region. This Arrhenius plot is clearly nonlinear; however, similar curvature for reduced Pd was also observed by Cant *et al.* (*5*). The average E_{app} value (21 ± kcal/mole) over the entire

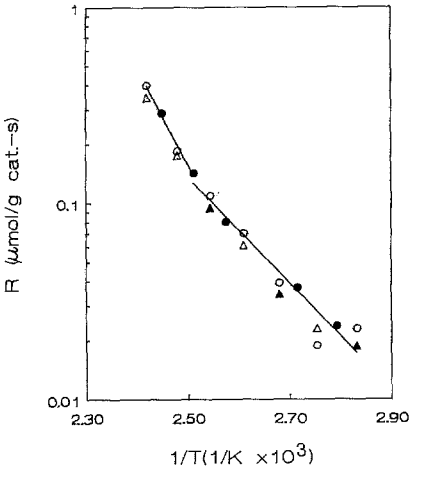

FIG. 1. Arrhenius plot for prereduced 2.19% Pd/δ-Al_2O_3 in the IR reactor. Total pressure = 750 Torr, P_{CO} = 26 Torr, P_{O_2} = 132 Torr; balance was He; Run 1, circles; Run 2, triangles; open symbols, ascending temp.; closed symbols, descending temp.

temperature range was higher than those obtained previously at lower temperatures, but at temperatures below 400 K, E_{app} was near 10 kcal/mole whereas near 450 K it was 30 kcal/mole. Thus, there is consistency among the various E_{app} measurements. The significance of this change in activation energy is discussed in detail later.

The partial pressure dependencies on each reactant were determined, and the various regimes are given in Table 3. At 373 K and a relatively high O_2 pressure of 132 Torr, the partial pressure dependency on CO was negative (−0.3), which is consistent with previous trends for the noble metals, while at 373 K and below the dependency on O_2 was 0.2 in the high pressure range and near first order in the lower pressure range, as shown in Fig. 3. The variations in the dependencies on CO and O_2 with temperature are shown in Figs. 3 and 4. At 343 K, the dependency on CO went through a shallow maximum and thereafter continually became more negative with increasing temperature, as indicated in Table 3 and Fig. 3a. With O_2, a near first-order dependency occurred in the lower pressure region, but the highest pressure to which this first-order regime extended continually decreased as the temperature increased. As temperature increased, the dependency in the higher pressure region continuously increased from 0.2 to 0.4 and this region was extended to lower pressures. Above 403 K, only a single dependency was observed and it increased with temperature to a value in the vicinity of one-half, as shown in Table 2.

All IR spectra were taken under a flowing gas mixture containing from 0.6 to 78 Torr CO, with 26 Torr representing the pressure at standard conditions. A typical IR spectrum for CO in He at 303 K gave CO bands at 2080, 1970, and 1925 cm^{-1}, as shown in Fig. 5. The 2080 and 1925 cm^{-1} peaks were strong while the 1970 cm^{-1} peak appeared as a shoulder. The intensity of the 2080 cm^{-1} peak decreased and the peak position shifted to 2070 cm^{-1} as the temperature increased; however, the 1970 peak intensity and position were independent of temperature while the intensity of the 1925 cm^{-1} peak also decreased and shifted toward 1910 cm^{-1} as the temperature increased. Under

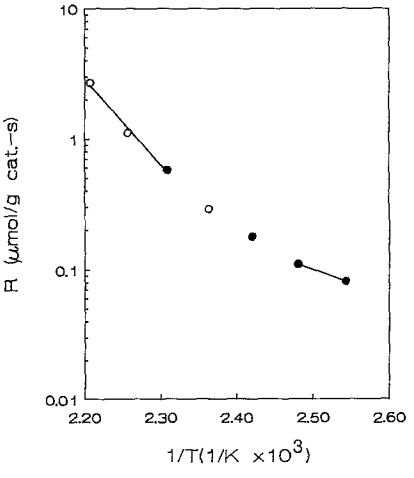

FIG. 2. Arrhenius plot for prereduced 2.19% Pd/δ-Al_2O_3 in the microreactor. Total pressure = 750 Torr, P_{CO} = 26 Torr, P_{O_2} = 132 Torr; balance was He; open symbols, ascending temp.; closed symbols, descending temp.

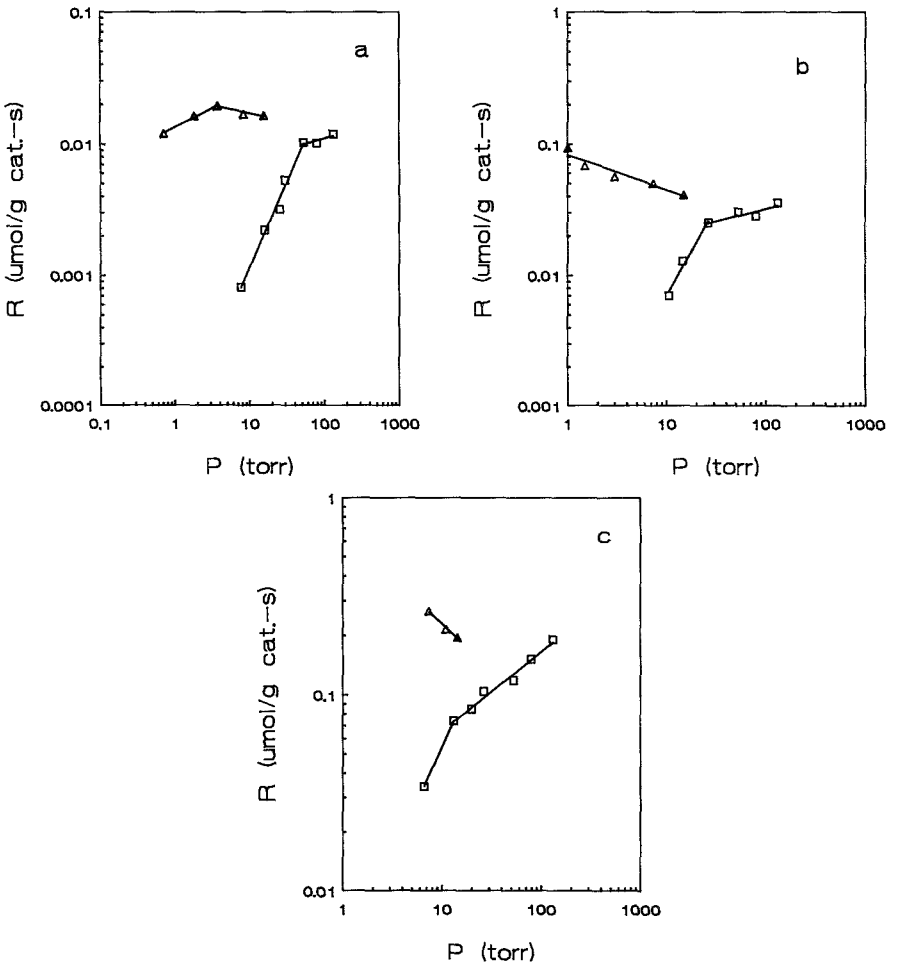

FIG. 3. Partial pressure dependencies on CO (△) and O_2 (□) over prereduced 2.19% Pd/δ-Al_2O_3 in the microreactor. (a) 343 K; (b) 373 K; (c) 403 K; gas flow = 28.5 cm^3/min, total pressure = 750 Torr, P_{CO} = 26 Torr when P_{O_2} varied; P_{O_2} = 132 Torr when P_{CO} varied.

standard reaction conditions with 132 Torr O_2 in the gas stream, the CO bands at 2080, 1970, and 1925 cm^{-1} were still observed and the 1970 and 1925 cm^{-1} peaks still overlapped, as shown in Fig. 6, but the latter band was the stronger of the two. As with CO in He, the position of the 2080 cm^{-1} band shifted down to 2065 cm^{-1} and its intensity decreased as the temperature increased from 303 to 413 K. As in He, the 1925 cm^{-1} peak of CO decreased in intensity and shifted again to 1910 cm^{-1} as the temperature increased, but the position and intensity of the 1970 cm^{-1} peak again remained nearly independent of the temperature.

During the partial pressure runs at 373 K in the IR reactor to determine rate dependencies on CO and O_2, the IR spectra in Figs. 7 and 8 were obtained. At the lowest CO pressure (1.1 Torr), strong CO peaks at 1970 and 1925 cm^{-1} were observed with the broad 1925 cm^{-1} peak initially being stronger, and only a very small linearly adsorbed CO peak was detected, as shown in Fig. 7. As the CO partial pressure increased, the 1970 and 2080 cm^{-1} peaks increased noticeably but little change in position oc-

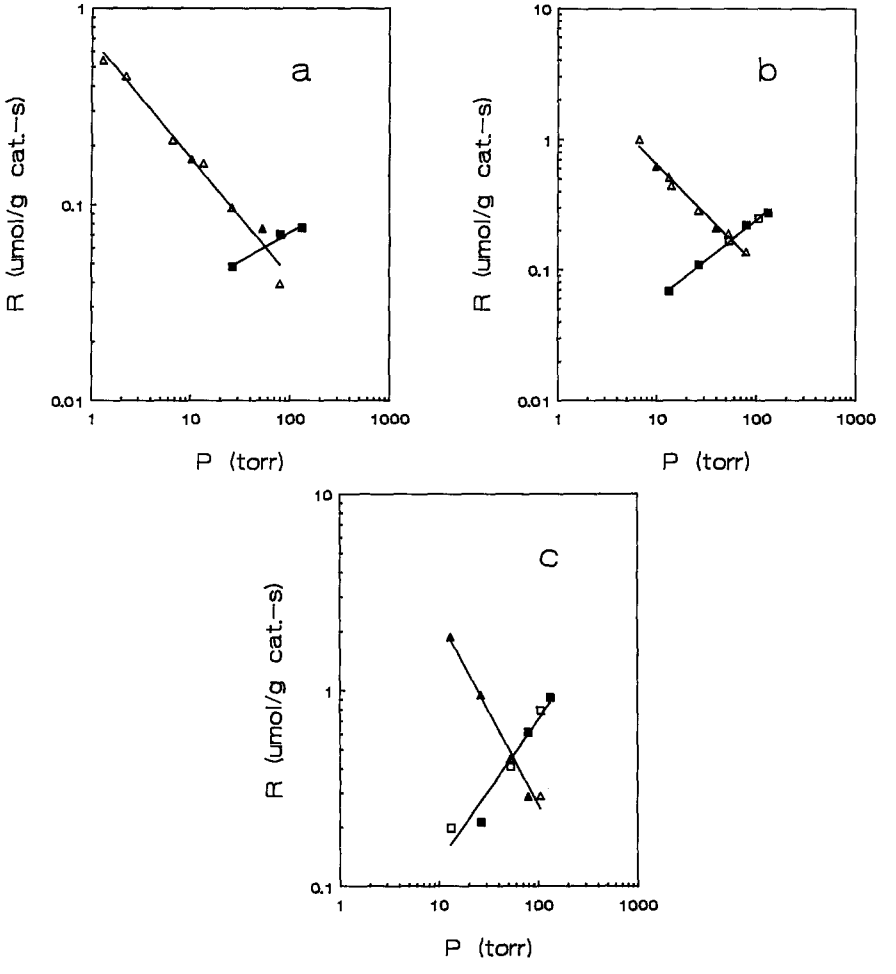

FIG. 4. Partial pressure dependencies on CO (△, ▲) and O_2 (□, ■) over prereduced 2.19% Pd/δ-Al_2O_3 in the microreactor. (a) 403 K; (b) 423 K; (c) 443 K; gas flow = 28.5 cm^3/min, total pressure = 750 Torr, P_{CO} = 26 Torr when P_{O_2} varied; P_{O_2} = 132 Torr when P_{CO} varied; open symbols, increasing P; closed symbols, decreasing P.

curred. As the O_2 partial pressure increased, the intensity the 1970 cm^{-1} CO band increased somewhat and sharpened, as shown in Fig. 8. Based on the work of Bradshaw and Hoffmann (*28*), this is an indication that the formation of a more compactly adsorbed CO species occurs on the surface, i.e., islands of compressed CO, when extensive oxygen adsorption exists on the Pd surface. Little change in the 2080 cm^{-1} band occurred. After these partial pressure runs, IR spectra under standard reaction conditions were remeasured, as shown in Fig. 9. They are similar to those shown in Fig. 6, with the most noticeable differences being the appearance at 303 K of an additional peak at 2150 cm^{-1} and a slightly stronger 1970 cm^{-1} band, relative to the 1925 cm^{-1} band, after these exposures to different O_2/CO ratios.

During the CO oxidation reaction within certain ranges of CO concentration and temperature, stable oscillatory behavior in both the amount of CO chemisorbed on the Pd and the rate of CO_2 formation was observed, as demonstrated in Figs. 10 and 11. As

TABLE 2

Catalytic Activities and Apparent Activation Energies for CO Oxidation over Prereduced $Pd/\delta\text{-}Al_2O_3$

Catalyst	E_{app}[a] (kcal/mole)		Activity[a] at 400 K (μmole CO/g cat · s)	TOF[a,b] (s^{-1})
	Below 400 K	Above 400 K		
2.10% $Pd/\delta\text{-}Al_2O_3$ (Reactor)	11.0 ± 0.2	16.0 ± 0.5	0.25	7.9×10^{-3}
2.10% $Pd/\delta\text{-}Al_2O_3$ (IR)	10.6 ± 0.1	20.7 ± 0.2	0.34 (extrapolated)	8.7×10^{-3}
2.19% $Pd/\delta\text{-}Al_2O_3$ Run 1	12.4 ± 0.1	22.8 ± 0.5	0.14	4.0×10^{-3}
(IR) Run 2	11.6 ± 0.1	22.3 ± 0.8	0.11	3.3×10^{-3}
2.19 $Pd/\delta\text{-}Al_2O_3$ (Reactor)	9.7 ± 0.1	17.3 ± 0.4	0.15	2.4×10^{-3}
2.19% $Pd/\delta\text{-}Al_2O_3$ (Reactor)	9.5 ± 0.1	30.2 ± 5.7[c]	0.10	1.7×10^{-3}
2.33% $Pd/\eta\text{-}Al_2O_3$ (Reactor)	12.6 ± 0.1		0.21 (extrapolated)	3.3×10^{-3}

[a] Standard reaction conditions: P_{O_2} = 132 Torr, P_{CO} = 26 Torr, total P = 750 Torr, values with 95% confidence limits.

[b] TOF = molecule CO reacted per second per surface Pd atom, T = 400 K.

[c] Obtained above 433 K.

shown in Fig. 10, at 403 K and 1400 ppm of CO (1.1 Torr CO) the amount of CO adsorbed on the Pd surface, as monitored by the principal 1910 cm^{-1} band, oscillated with a period of about 6 min, and the degree of CO_2 production varied in such a fashion that the maximum rate occurred at the lowest surface concentration of CO. The kinetic behavior could not be monitored as easily as the CO surface concentration because 25 min was required for each GC analysis. At a higher CO concentration (2000 ppm), the period of oscillation was prolonged to approximately 10 min and the trend of oscillation in CO_2 production was the same as observed at the lower CO concentration, i.e., higher activity at lower CO coverage. The oscillatory behavior was dependent not only

TABLE 3

Partial Pressure Dependencies on CO(X) and O_2(Y) for CO Oxidation over Prereduced 2.19% $Pd/\delta\text{-}Al_2O_3$

	X[a]	O_2/CO Ratio	Y[a]	O_2/CO Ratio	Temp. (K)
IR reactor	−0.3	1.7–174	0.2 (P_{O_2} > 26 Torr)	1–5	373
			1.4 (P_{O_2} < 26 Torr)	0.6–1	
Microreactor	0.3 (P_{CO} < 13 Torr)	35–182	0.2 (P_{O_2} > 52 Torr)	2–5	343
Sample I	−0.1 (P_{CO} > 13 Torr)	8–35	1.3 (P_{O_2} < 52 Torr)	0.3–2	
	−0.3	5–129	0.2 (P_{O_2} > 26 Torr)	1–5	373
			1.3 (P_{O_2} < 26 Torr)	0.4–1	
	−0.5	5–18	0.4 (P_{O_2} > 13 Torr)	0.5–5	403
			1.1 (P_{O_2} < 13 Torr)	0.25–0.5	
Sample II	−0.6	1.7–100	0.3	1–5	403
	−0.8	1.7–20	0.6	0.5–5	423
	−1.0	0.8–5	0.7	0.5–5	443

[a] $r = kP_{CO}^{X}P_{O_2}^{Y}$, P_{CO} = 26 Torr when Y was obtained, P_{O_2} = 132 Torr when X was obtained. Uncertainties as represented by 95% confidence limits were ±0.1 or better.

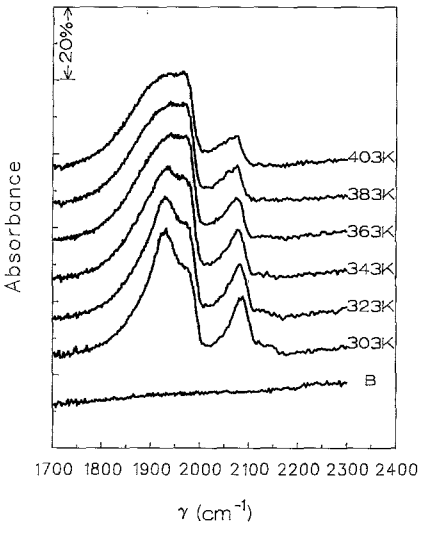

FIG. 5. IR spectra for prereduced 2.19% $Pd/\delta\text{-}Al_2O_3$ for CO in He only at various temperatures. Gas flow = 28.5 cm^3/min; total pressure = 750 Torr; P_{CO} = 26 Torr; balance was He.

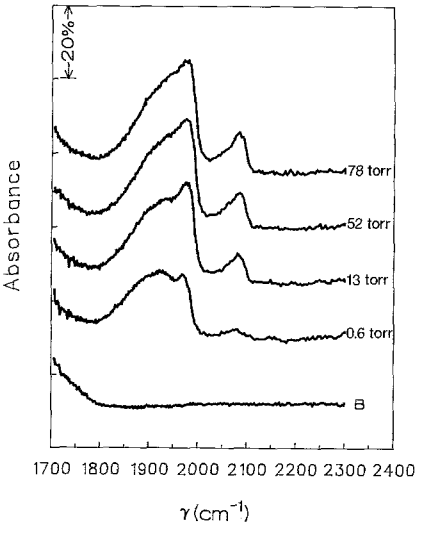

FIG. 7. IR spectra for prereduced 2.19% $Pd/\delta\text{-}Al_2O_3$ under reaction conditions at various CO partial pressures: T = 373 K; gas flow = 28.5 cm^3/min; total pressure = 750 Torr; P_{O_2} = 132 Torr; balance was He.

on CO concentration but also on temperature, and Fig. 11 shows that the higher the temperature, the shorter the oscillation period with 500 ppm CO (0.4 Torr) in the gas stream.

DISCUSSION

Steady-State Infrared Spectra

Bradshaw and Hoffmann have reported IR bands of CO chemisorbed on the (100),

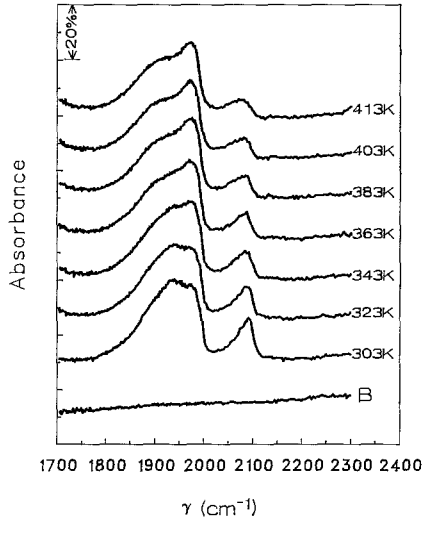

FIG. 6. IR spectra for prereduced 2.19% $Pd/\delta\text{-}Al_2O_3$ under standard reaction conditions at different temperatures: Gas flow = 28.5 cm^3/min; total pressure = 750 Torr; P_{CO} = 26 Torr; P_{O_2} = 132 Torr; balance was He.

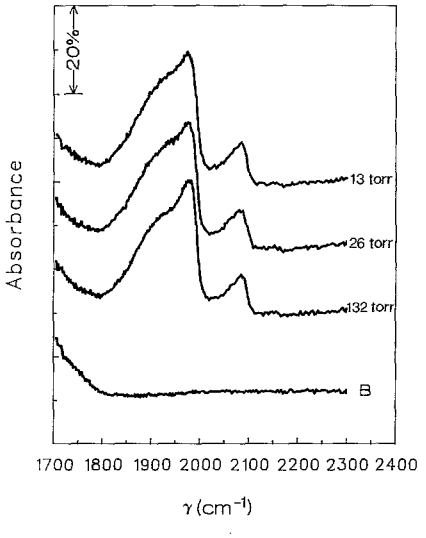

FIG. 8. IR spectra for prereduced 2.19% $Pd/\delta\text{-}Al_2O_3$ under reaction conditions at various O_2 partial pressures: T = 373 K; gas flow = 28.5 cm^3/min; total pressure = 750 Torr; P_{CO} = 26 Torr; balance was He.

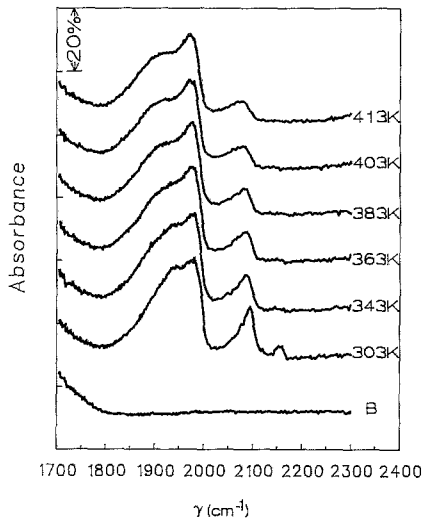

FIG. 9. Sequential IR spectra for prereduced 2.19% $Pd/\delta\text{-}Al_2O_3$ at various temperatures and standard reaction conditions after CO and O_2 partial pressure runs. Gas flow 28.5 cm^3/min; total pressure = 750 Torr; P_{O_2} = 26 Torr; P_{O_2} = 132 Torr.

(111), and (210) single-crystal surfaces of Pd (*28*). Their work showed that CO on Pd(100) at 300 K and low coverage has a band at 1895 cm^{-1} which shifts gradually to 1930 cm^{-1} at a coverage near $\theta = 0.4$ and then rapidly to 1983 cm^{-1} at $\theta = 0.61$. The rapid change of frequency at high coverage was attributed to the formation of "compressed CO" (or CO islands) in which the increased dipole–dipole interaction increases the wave number. In the region below the compression regime ($\theta < 0.5$), LEED data (*29*) strongly indicate the existence of a twofold coordinated (bridged) species which provides the initial band at 1895 cm^{-1} and is responsible for the rapid shift from 1930 cm^{-1} at $\theta = 0.5$ to 1983 cm^{-1} during compression. For CO on Pd(111), similar behavior was observed as the band is at 1823 cm^{-1} at low coverage, increases smoothly to 1836 cm^{-1} at $\theta = 0.33$, and then rapidly shifts to 1946 cm^{-1} at higher coverages. The appearance of an additional band at 2092 cm^{-1} for

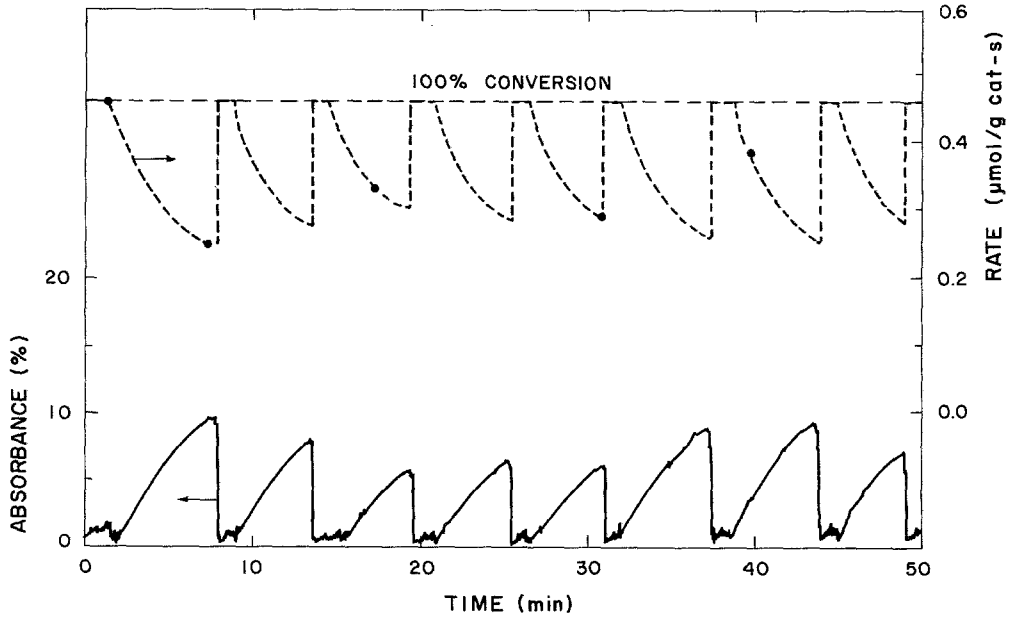

FIG. 10. Oscillatory behavior of the activity and the concentration of adsorbed CO on 2.19% Pd/Al_2O_3 monitored by the 1910 cm^{-1} peak intensity: T = 403 K; P_{O_2} = 132 Torr; P_{CO} = 1.1 Torr (1400 ppm). Total pressure = 750 Torr, balance was He.

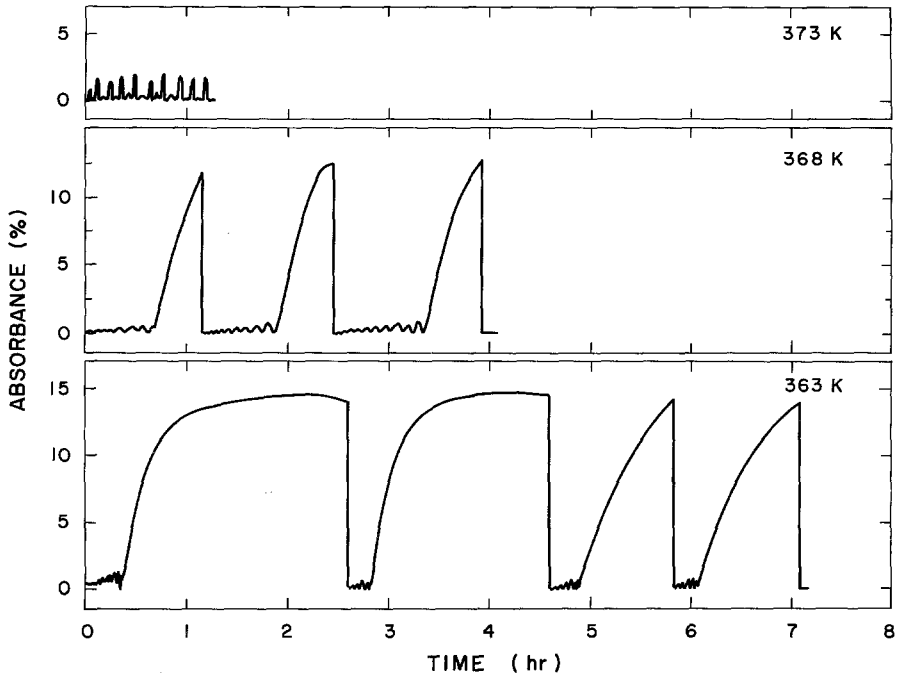

FIG. 11. Oscillatory behavior of the concentration of adsorbed CO on 2.19% Pd/Al_2O_3 monitored by the 1910 cm^{-1} peak intensity at 363, 368, and 373 K; P_{O_2} = 132 Torr; P_{CO} = 0.4 Torr (500 ppm). Total pressure = 750 Torr, balance was He.

linearly adsorbed CO also occurs at high coverage. This sequence of spectra was interpreted in terms of adsorption first on threefold coordination sites (1820 to 1840 cm^{-1}), then on twofold coordination sites (1890 to 1946 cm^{-1}) through a transition region where both twofold and threefold coordinated species are present. The linear CO species observed at 2092 cm^{-1} was considered to be CO terminally adsorbed on a single Pd atom. With Pd(210), which has a more open structure in the top layer, they found the spectra increased from 1878 cm^{-1} at low coverage to 1940 cm^{-1} at a coverage near 0.5, then shifted more rapidly to 1996 cm^{-1} at high coverage. This behavior is quite similar to that described previously and is interpreted in a similar manner.

A number of IR studies have been conducted on CO chemisorbed on supported Pd catalysts (*19, 20, 30–36*). The assignment in the original studies of Eischens and coworkers (*31, 32*) of terminally bonded (linear) CO to the high frequency band above 2050 cm^{-1} and of multiply coordinated (bridgebonded) CO to the lower frequency bands below 2000 cm^{-1} has been confirmed in subsequent investigations. Although various lower frequency peaks between 1990 and 1800 cm^{-1} have been observed by different investigators, as summarized elsewhere (*36*), they can be associated with the different species proposed by Bradshaw and Hoffmann (*28*). Fresh reduced catalysts sometimes exhibit different variations in peak intensities with CO coverage than catalysts after exposure to CO and O_2 at higher temperatures (*30–34*). However, changes in the distribution of crystal planes due to surface restructuring and sintering during this "break-in" period can be proposed to straightforwardly explain this. The typical

trend is a shift in intensity from the region between 1800 and 1940 cm^{-1} to a region between 1950 and 1990 cm^{-1} after this break-in period, which is consistent with a loss of high index planes to form the more stable low index planes (*30*). Palazov *et al.* also showed that oxidation of the Pd surface gave bands at 2103 and 2135 cm^{-1} at saturation coverage, and after a high temperature treatment in O_2 at 723 K, no bridge-bonded CO species were observed (*33*).

The spectra of adsorbed CO obtained in the present study are in general quite similar to those obtained by Palazov *et al.* (*33*) for Pd/Al_2O_3, and by Baddour *et al.* (*19*) and Kember and Sheppard (*20*) for Pd/SiO_2. The assignments from these previous studies are used here; therefore, the 2080 cm^{-1} band is that of CO linearly bonded to a surface atom and the bands at 1925 and 1970 cm^{-1} represent bridged species bound to two Pd_s atoms. At the CO pressures used here, coverages on the Pd surfaces should be high and the 1925 and 1970 cm^{-1} bands can be associated with compressed CO phases on the (111) and (100) surfaces, respectively. This interpretation is supported by the IR work of Boecker and Wicke (*37*), which showed a sharp absorption band centered at 1980 cm^{-1} when the CO island size was increasing, and the EELS study of Stuve *et al.* which resolved a CO peak near 1990 cm^{-1} at CO coverages over one-half on a Pd(100) surface covered with 0.25 monolayer of oxygen (*12*).

The development of CO bands after CO adsorption on a Pd surface partially covered by oxygen was also examined in this study, as shown in Fig. 12. Initially the surface was covered by oxygen, then 500 ppm of CO (0.4 Torr CO) was introduced into the system at 373 K. A strong, broad peak centered at 1925 cm^{-1} developed first along with the bands for linear CO, and the 1970 cm^{-1} peak was initially only a shoulder; however, the 1970 cm^{-1} band grew continuously. A peak at 2140 cm^{-1} was also observed during the first two scans. In the IR spectra taken during the CO partial pressure runs (Fig. 7), the 1925 cm^{-1} peak again developed first and the 1970 cm^{-1} band grew in relative strength as both the CO pressure and time under reaction conditions increased. After these runs, the 1970 cm^{-1} peak had grown relative to the 1925 cm^{-1} band (compare spectra in Fig. 9 and 6). Upon exposure of an O-covered Pd/SiO_2 sample to CO, Li *et al.* saw the growth of bands at 1932 and 1978 cm^{-1} beginning at the same time, with the intensity of the latter being favored and continuing to grow over a longer period of time (*38*). Although Fig. 12 could imply different rates on certain planes like the (100) surface because of the slower development of the 1978 cm^{-1} peak, it more likely indicates that some surface refacetting to the (100) plane occurs under reaction conditions. This latter explanation is consistent with the changes associated with a break-in period (*20*) and with the results showing this reaction is structure insensitive (*39, 40*).

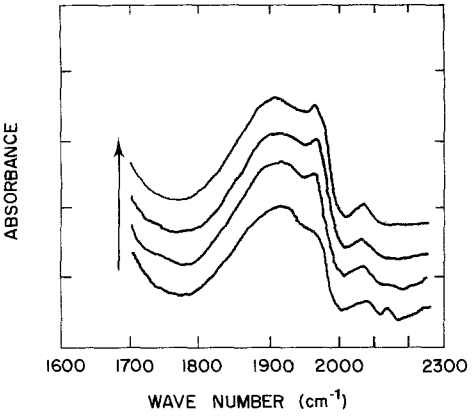

FIG. 12. Variation with time of IR spectra of CO on oxygen-covered 2.19% $Pd/\delta\text{-}Al_2O_3$ after initiating CO flow. Each scan required 5 min, and arrow indicates increasing time. T = 373 K; total pressure = 750 Torr; P_{CO} = 0.4 Torr; P_{O_2} = 132 Torr, balance was He.

The state of the Pd surface at 373 K under various reaction conditions, as monitored by the adsorbed CO species, and the dependence of the rate on these different CO spe-

cies can be seen in Figs. 7 and 8. In Fig. 7 all CO peak intensities decrease as CO pressure decreases, especially the 2080 cm^{-1} peak, but the rate increases threefold. The most obvious interpretation is that a decrease in adsorbed CO as the CO pressure drops is freeing up surface sites and facilitating the competitive adsorption of oxygen. The coverage decreases more rapidly as the CO pressure decreases below 10 Torr. The invariance of the CO band intensities in Fig. 8 as both O_2 pressures and rates decrease is again consistent with this picture, and the sharpening of the 1970 cm^{-1} band as O_2 pressure increases can be explained by the increased compression of CO islands as the amount of adsorbed oxygen grows because little or no CO is displaced at this high CO pressure. All these trends are consistent with the zero-to-negative-order dependence on CO at CO pressures above 1 Torr.

Oscillatory IR/Kinetic Behavior

Many studies have now addressed the oscillations in rate and CO coverage that can occur during the CO oxidation reaction over noble metals (*41*), and numerous explanations have been provided to explain this behavior. These include heat transfer effects (*16*), surface restructuring (*42, 43*), redox of surface atoms (*44, 45*), mass transfer limitations (*46, 47*), and carbon deposition (*48, 49*). Although Pt has been the most widely studied metal system, these oscillations have also been observed during CO oxidation over Pd (*15–17, 46*). The intent of the present investigation was not to study oscillatory behavior and, in fact, efforts were made to avoid it because steady-state behavior was desired. However, the observation of these oscillations with Pd/Al_2O_3 is briefly mentioned here because it represents only the second case reported for supported Pd, and the oscillations occurred at much lower CO concentrations than that used by Kaul and Wolf (*16*).

Although oscillations in the surface concentration of CO under reaction conditions could be followed readily by continuously monitoring the peak intensity at 1910 cm^{-1}, CO_2 formation could not be followed continuously because gas chromatography was used for exit gas analysis. However, if the inverse correlation between activity and CO surface coverage that normally occurs was assumed to exist, as Kaul and Wolf have shown for Pd (*16*), then the rate oscillations could be predicted from the IR data. GC analyses were made at different CO coverages to test rate behavior, and the results in Fig. 10 show the fit is excellent and the expected inverse dependence does indeed exist. The CO conversion at this CO concentration of 1400 ppm is clearly not differential as it varies between 50 and 100%. The fact that these oscillations occur at this and even lower CO concentrations (see Fig. 11), which are 50 to 100 times lower than that used by Kaul and Wolf, would tend to argue against heat transfer limitations being the cause of these oscillations but would be consistent with a surface restructuring process similar to that for Pt, as suggested in (*16*). However, these oscillations were observed in the regime where islands of reactants appear to exist, and Mukesh *et al.* have shown that a surface in such a state can produce oscillatory behavior (*14*). This consequently represents another explanation.

Reaction Model for CO Oxidation

Many kinetic studies of the reaction between CO and O_2 have been conducted, and it has been found that the form of the kinetic expression describing the rate of CO oxidation over Pd is very dependent upon temperature and reactant pressures (*1–7, 11, 50–68*). The studies of Engel and Ertl, involving very low pressures of both CO and O_2, clearly eliminated a Rideal–Eley mechanism and delineated four different regimes involving a bimolecular surface reaction (routinely designated as a Langmuir–Hinshelwood mechanism), each of which can have a different rate expression (*2*). These and two other regimes can be summarized as follows: (1) at very low coverages of adsorbed reactants (low θ_{CO} and θ_O) and with

adsorption equilibrium established (favored at $T > 500$ K), the Langmuir–Hinshelwood rate expression simplifies to $r = kP_{CO}P_{O_2}^{1/2}$ (*2*); (2) if P_{O_2} is too low, then $r = kP_{O_2}$ because the rate-determining step (rds) shifts to O_2 adsorption (*2*); (3) at higher P_{CO} where θ_{CO} becomes significant, O_2 adsorption can be hindered, and one limiting case at high θ_{CO} values when O_2 adsorption via a molecular precursor state is the slow step gives $r = kP_{O_2}P_{CO}^{-1}$— this is the expression most frequently reported and typically found below 500 K and at low pressures (*2, 4*); (4) if $P_{CO} \ll P_{O_2}$ so that θ_{CO} is very small and the rate becomes independent of O_2, then $r = kP_{CO}$ (CO diffusion on the surface to react with islands of oxygen adatoms has also been proposed in this regime (*2*)); (5) at lower temperatures and higher O_2 pressures when the rds is the reaction between randomly adsorbed O atoms and adsorbed CO molecules, the normal L–H rate expression applies; and (6) at certain pressures of CO and O_2, islands of compressed oxygen adatoms exist as well as compressed domains of CO, and the reaction occurs at the perimeter of these islands (*2, 12, 14, 69*). Consequently, as others have stated (*2, 68*), a single reaction mechanism cannot describe this reaction over wide ranges of temperature and pressure.

Previous studies have reported kinetic behavior consistent with these various regimes. Ladas *et al.* examined this reaction at low pressures (ca. 10^{-6}–10^{-1} Torr) over Pd sputtered onto an α-Al_2O_3 single crystal and their results fit regime 3 at 448 K (*6*). Cant *et al.* studied CO oxidation at higher pressure over a Pd/SiO_2 catalyst and reported a rate expression of $r = P_{O_2}^{0.9}P_{CO}^{-0.8}$ above 427 K, Berlowitz *et al.* found reaction orders of 1 and -1 in O_2 and CO, respectively, on Pd(110) at 525 K as long as the O_2/CO ratio was less than 12 (*7*), and Yao reported similar dependencies for a series of Pd/Al_2O_3 catalysts at 523 K (*60*). Consequently, most of the reported rate expressions appear to fall in regime 3, as indicated in Table 4, although Berlowitz *et al.* observed a transition to regime 5 (*7*). In region 3; if O_2 adsorption is an irreversible step then $k = k_{ad}/K_{CO}$, where k_{ad} is the rate constant for O_2 adsorption and K_{CO} is the equilibrium adsorption constant for CO; thus the apparent activation energy (E_{app}) is equal to $E_{ad} + Q_{CO}$, the activation energy for O_2 adsorption and the heat of adsorption for CO, respectively (*2, 40*). As E_{ad} is expected to be zero or near zero, at least for clean surfaces, E_{app} should be close to Q_{CO} on Pd. Although E_{app} values have frequently fallen between 25 and 30 kcal/mole, a much wider range has been reported, as shown in Table 4. Lower Q_{CO} values on CO-covered surfaces could explain somewhat the lower E_{app} values (*40*), but this wide range is most likely due to the different combinations of rate parameters that occur in various regimes although the possibility of activated O_2 adsorption has been mentioned (*40*). Finally, it is important to note that an activation energy of 25 kcal/mole has been measured for the reaction between an oxygen atom and a CO molecule on Pd(111) at very low pressures corresponding to regimes 3 and 4, and it decreases to 14 kcal/mole when the compressed oxygen islands in regime 6 are formed (*2*).

Under conditions where the limiting case in regime 3 is applicable, that is, $r = kP_{O_2}/P_{CO}$, the rate should be independent of total pressure at an equimolar reactant ratio; however, Landry *et al.* (*68*) have reported a sevenfold increase in turnover frequency at 445 K as the pressure increased from 10^{-6} to 100 Torr. Consequently, the turnover frequencies in Table 2 are quite consistent with those listed in Table 4 with the exception of those for TiO_2-supported Pd (*64*) and one of the catalysts studied by Vorontsov and Kasatkina (*58*).

The kinetic results in Table 3 show that in the lower pressure region, the near first-order dependency on O_2 and the negative dependencies on CO would indicate the presence of regime 3, i.e., $r = kP_{O_2}/(1 + K_{CO}P_{CO})$ (*4*). As the O_2 pressure increases, the system moves into regime 5 or 6, and it

TABLE 4

Kinetic Parameters Reported for CO Oxidation over Pd

Catalyst	E_{act} (kcal/mole)	T (K)	P_{CO} (Torr)	P_{O_2} (Torr)	TOF at 400 K ($s^{-1} \times 10^3$)	X^a	Y^a	Ref.
Pd(111)	25	450–700	1×10^{-7}	4×10^{-7}	—	−1	1	(*2, 3*)
	18	480–700	3×10^{-7}	4×10^{-7}	—			
	14	530–700	1×10^{-6}	4×10^{-7}	2.2			
Pd/α-Al_2O_3	—	448	5×10^{-7}	5×10^{-7}	1[b]	−1	1	(*6*)
5% Pd/SiO_2	24.6	400–450	9.8	4.9	1	−0.8	0.9	(*5*)
Pd(110)	33.1	475–625	16	130	2[b]	−1.0	1.0	(*7*)
	26.0	<460						
0.13% Pd/κ-Al_2O_3	30	463–523	20	10	5	—	—	(*58*)
0.5% Pd/κ-Al_2O_3	21.9	453–498			31			(*58*)
1.2% Pd/κ-Al_2O_3	25.9	433–508			5			(*58*)
10% Pd/SiO_2	30	383–443	17	12				(*19*)
Pd/Al_2O_3	13–32	>473	$P_{CO}/P_{O_2} = 1$			−1	1	(*60*)
Pd foil	22.2	523–593	—			—	—	(*61*)
Pd/α-Al_2O_3	28.5	473–523				—	—	(*62*)
0.5% Pd/α-Al_2O_3	25.1	473–523				—	—	(*63*)
	7.7	343–473						
0.5% Pd/SiO_2	37.0	463–513	2	1				(*63*)
0.5% Pd/MgO	34.7	523–623						(*63*)
9% Pd/TiO_2	9.6	293–323	150	75	66	0.3	0	(*64*)
2% Pd/SiO_2	19.9	Around 453 K	46	152		−1	1	(*65*)
1% Pd/SnO_2	14.1	Around 384 K	46	152		0	0.5	(*65*)
1.3% Pd/SnO_2	9.9	246–317	60	30		—	—	(*66*)
Pd/$LiNbO_3$	30.5[c]	493–673	20	10		−1	1	(*67*)
	23[d]							
4.88% Pd/Al_2O_3	26.8	420–450	41	42	2.4	—	—	(*68*)
	18.4	420–450	0.75	0.83	1.9			

[a] $r = kP_{CO}^X P_{O_2}^Y$.
[b] Extrapolated value (33.1 kcal/mole).
[c] 0.2-mm Pd film.
[d] 0.02-mm Pd film.

is only this higher O_2 pressure region that will be modeled because the activation energies and most of the IR spectra were obtained under these conditions. If a surface reaction between adsorbed O atoms and CO molecules is chosen to interpret the results in Tables 2 and 3 at higher O_2 pressures, then the following comments can be made based on the previous discussion. Under standard reaction conditions ($P_{O_2}/P_{CO} = 5$), the low activation energies of 10–11 kcal/mole below 380 K and the CO bands at 1925 and 1970 cm^{-1} imply reaction between compressed domains of CO and compressed islands of oxygen. The higher values above 20 kcal/mole at temperatures close to 450 K would indicate a reaction between CO and "normal" oxygen atoms which are not in compressed islands (*2*), perhaps similar to the mixed phase reported by Matsushima and Asada (*69*). The transition appears to occur around 400 K. High CO coverages exist over the entire temperature range because the pressure dependencies in Table 3 vary from near zero order at 343 K to negative first order at 443 K. In the higher pressure region, oxygen dependencies are near 0.2 at lower temperatures and increase to

slightly over one-half as temperature increases. Thus regime 5 appears most reasonable at the highest temperatures and regime 6 may be more appropriate at the lower temperatures. Figures 3 and 4 show these patterns.

Stuve *et al.* examined this reaction on an O-covered Pd(100) surface and reported three different reaction regimes (*12*). Between 100 and 300 K, CO_2 formation occurred via CO–Pd–O complexes (with a band frequency of 2125 cm^{-1}); at 360 K CO_2 formed from the reaction of adsorbed CO with disordered oxygen domains; and at 420 K the reaction occurred between adsorbed CO and isolated O atoms (or an ordered $p(2 \times 2)$ oxygen layer). The transition between the last two regions as the temperature increased matches that found in the present study, as indicated by the shift in E_{app} values. Zhou and Gulari have also observed an adsorbed CO species under transient conditions with a band frequency of 2156 cm^{-1} whose concentration correlated with CO_2 formation (*70*). At lower temperatures we have also observed this species (Fig. 12); thus this may represent the complex mentioned above. Finally, the reaction between domains of CO and compressed islands of oxygen as well as the reaction between CO molecules and O atoms in a mixed structure has been reported by Matsushima and Asada for the Pd(111) surface (*69*).

The IR spectra obtained during reaction show that surface concentrations of CO are high up to the highest temperature studied (413 K), and the largest rates during oscillatory behavior occurred at the lowest CO coverage. As mentioned previously, the spectra in Figs. 7 and 8 also showed this trend. Thus all results are in agreement with the negative pressure dependencies that were measured. The presence of the 1970 cm^{-1} peak during reaction and its relative enhancement at higher CO pressures (Fig. 7) indicate the existence of compressed domains of CO (*28*). Consequently, the IR results suggest the kinetic model for regime 6 is applicable, i.e., the reaction of adsorbed CO and O atoms at the interface of domains of CO and islands of oxygen atoms. The existence of this model in the temperature region below 400 K is also implied by the low activation energy and the reaction orders near -0.5 in CO and near 0.25 in O_2, as discussed shortly. At higher temperatures, the partial pressure dependencies are better fit by the traditional L–H model (regime 5). However, a rate equation is derived from each model and applied to the data, then the quality of fit and the values of the fitted parameters are analyzed to see which appears most appropriate. Presumably because of the lower temperatures and high pressures, especially for O_2, the pressure dependencies found here differ from those that exist in the more frequently observed regime 3.

In either the typical L–H model or the island model, the surface reaction between an adsorbed CO molecule and an adsorbed oxygen atom is assumed to be the rate-determining step, and both CO and O_2 adsorption are then in quasi-equilibrium. The sequence of elementary steps for the L–H model is then

$$CO + * \overset{K_{CO}}{\rightleftharpoons} CO* \tag{2}$$

$$O_2 + 2* \overset{K_{O_2}}{\rightleftharpoons} 2O* \tag{3}$$

$$CO* + O* \xrightarrow{k} CO_2 + 2* \text{ (rds)}, \tag{4}$$

where CO* is an adsorbed CO molecule, O* is an adsorbed oxygen atom, and * is a vacant site. The standard L–H equation for bimolecular reactions is then attained,

$$r = \frac{kK_{CO}P_{CO}\sqrt{K_{O_2}P_{O_2}}}{(1 + K_{CO}P_{CO} + \sqrt{K_{O_2}P_{O_2}})^2}, \tag{5}$$

where K_{CO} and K_{O_2} are equilibrium adsorption constants.

The appropriateness of step 3 might be questioned because at low O_2 pressures oxygen adsorption can be considered an irre-

versible step under reaction conditions (*2, 6*). However, at these high O_2 pressures this quasi-equilibrium would be favored and the rate dependencies on O_2 pressure in Fig. 3 exhibit the curvature at higher pressures expected for a bimolecular L–H reaction. These partial pressure dependencies are very similar to those observed by Berlowitz, *et al.* for a Pd(110) surface over the same pressure range but at higher temperatures, and this curvature away from a first-order dependence to a zero or negative dependence was attributed to the presence of oxygen on the surface (*7*). A sharp change from a region of lower activity, first-order O_2 dependence to a region of higher activity, zero-order O_2 dependence has been reported by Mishchenko *et al.* (*71*). Also, the high heat of adsorption of O_2 on Pd would produce very large K_{O_2} values that could approximate an irreversible step. Finally, the assumption of quasi-equilibrium for O_2 adsorption was made by Mukesh *et al.* (*14*) in their derivation of the island model, and it predicted catalytic performance and oscillatory behavior more accurately than the model making no assumptions about the relative rates in the elementary steps shown in (2)–(4). Therefore, there is evidence that this model may indeed be appropriate under certain reaction conditions, but these regimes are quite sensitive to temperature, pressure, and the O_2/CO ratio.

As mentioned earlier, once islands of adsorbed species are formed on the surface, the reaction can occur only along the perimeter of each island because the adsorbed species within the islands cannot interact with the other reactant. In their derivation of a rate expression based upon the model that both adsorbed reactants form islands, it was assumed by Cutlip and co-workers that the islands are circular and of the same size and the number of islands is constant; i.e., it is independent of the surface coverage (*14*). This results in a rate expression of the form

$$r = k' I_{CO} I_{O_2} = k'' \sqrt{\theta_{CO} \theta_O}, \qquad (6)$$

where I_{CO} and I_{O_2} are the total concentrations of CO molecules and oxygen atoms at the perimeters of their respective islands or domains, and substitution of the two Langmuir isotherms into Eq. (6) gives

$$r = \frac{k\sqrt{K_{CO} P_{CO} \sqrt{K_{O_2} P_{O_2}}}}{(1 + K_{CO} P_{CO} + \sqrt{K_{O_2} P_{O_2}})} \qquad (7)$$

as the rate expression derived for the model assuming both reactants exist in islands or domains (*14*).

Using the direct search simplex method, the constants k, K_{CO}, and K_{O_2} in Eqs. (5) and (7) were computed by fitting these equations to the partial pressure data. These results are given in Table 5, and predicted rate curves are compared with the data in Figs. 13 and 14. In the low temperature region below 400 K, the island model indeed represents the data better than the standard L–H expression, as shown in Fig. 13, whereas above 400 K the standard L–H model tends to provide a better fit, as shown in Fig. 14. Mukesh *et al.* (*14*) and Li *et al.* (*38*) found that the island model described their data well for Pt at 373 K and Pd at 353 K, and the reaction temperatures they used agree with the lower temperature region of applicability found in the present study. Values of θ_{CO} and θ_O can be estimated from the K_{CO} and K_{O_2} constants in Table 5, but it should be kept in mind these represent the fraction of active sites covered, and there may not be a 1 : 1 correspondence between active sites and adsorption sites. Regardless, for the runs in Fig. 13, θ_{CO} varies from 0.40 to 0.98 over the CO pressure range studied while θ_O values fall between 0.02 and 0.58. Thus a plausible range of coverages exists to allow islands of each species to form. Over the somewhat higher CO pressure range in Fig. 14, θ_{CO} varies from 0.87 to 0.99 while oxygen coverages are lower and fall between 0.01 and 0.12. The findings are also consistent with the fact that the island model can predict oscillations, and it was at temperatures of 403 K or lower than we obtained oscillations (Figs. 10 and 11).

TABLE 5

Computed Rate Parameters (k, K_{CO}, K_{O_2}) for Prereduced 2.19% Pd/δ-Al_2O_3

Sample	Reaction temp. (K)	Constants			ΔH^0_{ad} (kcal/mole)		ΔS^0_{ad} (cal/mole K)		E_{rds}[d] (kcal/mole)	A[d] (s^{-1})
		k (s^{-1})	K_{CO}[c]	K_{O_2}[c]	CO	O_2	CO	O_2		
IR Reactor[a]	373	0.27	1.0×10^5	1.0×10^5	—	—	—	—	—	—
Microreactor[a]	343	0.04	9.5×10^5	9.7×10^7						
I	373	0.15	1.7×10^5	5.6×10^5	−14	−42	−13	−87	15	1.0×10^8
	403	0.96	4.6×10^4	9.3×10^3						
Microreactor[b]	403	1.9	8.6×10^4	1.6×10^5						
II	423	8.5	3.8×10^4	1.2×10^4	−19	−45	−25	−88	23	1.4×10^{12}
	443	22	1.0×10^4	1.0×10^3						

[a] Constants were computed from island model (Eq. (7)).
[b] Constants were computed from L–H model (Eq. (5)).
[c] Based on units of atm^{-1} and a standard state of 1 atm.
[d] $k = A \exp(-E_{rds}/RT)$.

Since the island model fits the experimental data better in the low temperature region, it was utilized to compute the constants in Table 5. From these constants the activation energy for the rds and the heats of adsorption ($Q_{ad} = -\Delta H^0_{ad}$) for CO and O_2 were calculated to evaluate the physical consistency of these parameters. The activation energy for the rds in the temperature region below 400 K is 15 kcal/mole, and the computed heats of adsorption from the K_{CO} and K_{O_2} values are 14 and 42 kcal/mole, respectively. From the literature, estimated integral heats of adsorption for CO on Pd range from 16 to 33 kcal/mole (*29, 72–75*), and integral Q_{CO} values of 20–23 kcal/mole have been measured for CO on Pd/Al_2O_3 catalysts similar to those studied here (*26*). Thus the value of 14 kcal/mole for CO is reasonable, particularly when it applies to compressed CO domains which should have an even lower Q_{CO} value. Reported heats of

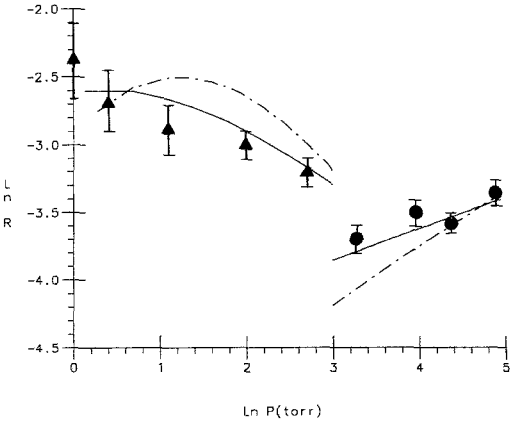

FIG. 13. Comparison between data and computed results from both the island (solid line) and the L–H (dashed line) models for CO oxidation over prereduced 2.19% Pd/δ-Al_2O_3 catalysts; (▲) CO, (●) O_2. Microreactor, T = 373 K. Estimated error bars are included.

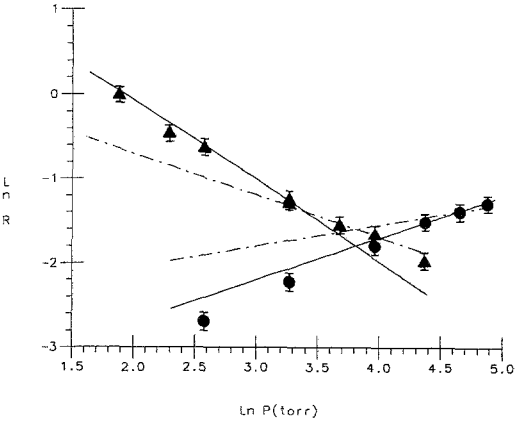

FIG. 14. Comparison between data and computed results from both the island (dashed line) and the L–H (solid line) models for CO oxidation over prereduced 2.19% Pd/δ-Al_2O_3 catalysts; (▲) CO, (●) O_2. Microreactor, T = 423 K. Estimated error bars are included.

adsorption for O_2 on Pd have varied from 40 to 80 kcal/mole (*76–82*), and integral values on Pd catalysts with crystallite sizes similar to those here were near 50 kcal/mole (*27*). Thus, the value of 42 is also very reasonable and a somewhat lower value might again be expected for compressed domains of oxygen. Perhaps even more satisfying is the agreement between the activation energy of 15 kcal/mole calculated here and that of 14 kcal/mole reported by Engel and Ertl in their molecular beam study of the reaction between domains of CO and compressed islands of oxygen (*2*). In addition, under their conditions they saw the oxygen islands disappear between 400 and 450 K, which is very close to the temperature range where we find the transformation at higher pressures.

In the temperature region above 400 K, the standard L–H model appears more appropriate and it was used to calculate these same parameters. The activation energy of 23 kcal/mole for the reaction between randomly adsorbed CO molecules and oxygen atoms is higher and quite close to the value of 25 kcal/mole expected from the literature in the absence of islands (*2*). The heats of adsorption for CO and O_2 computed from the K_{CO} and K_{O_2} values in Table 5—19 and 45 kcal/mole, respectively—are higher, consistent with the presence of noncompressed adsorbed species, and even closer to the integral values measured previously (*26, 27*). Thus the trends exhibited by these two models through an apparent kinetic transition region are extremely reasonable and lend support to the two proposed reaction models. It is also apparent why significant curvature can occur in the Arrhenius plots, as shown in Figs. 1 and 2 and as found in previous studies (*5, 7*), and, as stated previously, a single mechanism cannot describe this reaction under all conditions.

Finally, the low temperature regime in which a first-order O_2 dependency occurred has not been analyzed in detail here because no Arrhenius data were obtained under these lower pressure conditions. However, as mentioned previously, this behavior conforms to regime 3 where O_2 adsorption can be the slow step, and with this assumption the rate is $r = k_{ad}P_{O_2}/(1 + K_{CO}P_{CO})$ (*4*). Since rates were measured under these conditions at three different temperatures (Fig. 3) and constant O_2 and CO partial pressures, values for the ratio of k_{ad}/K_{CO} can be obtained if the rate dependency at high CO coverages, which is frequently obtained, is assumed, i.e., $r = k_{ad}P_{O_2}/K_{CO}P_{CO}$. At an O_2 pressure of 13 Torr and a CO pressure of 26 Torr, the apparent activation energy for k_{ad}/K_{CO} was near 18 kcal/mole. Under these conditions $E_{app} = E_{ad} + Q_{CO}$; consequently, since integral Q_{CO} values (and Q_{CO} values at high coverages) have been reported between 16 and 23 kcal/mole (*26*) it can be concluded that O_2 adsorption is essentially nonactivated on these CO-covered surfaces. If the dependency on CO is weaker than negative first order, as the data in Fig. 3 and Table 3 imply, then the more general L–H type rate expression, i.e., $r = k_{ad}P_{O_2}/(1 + K_{CO}P_{CO})$, must be used. With this approach, k_{ad} values at each temperature could be obtained by choosing a Q_{CO} value and estimating a value for K_{CO} (*83*); with Q_{CO} = 19 kcal/mole, which again is very close to reported integral values, a value of zero for E_{ad} was obtained thereby also indicating little or no activation barrier for O_2 adsorption on these CO-covered surfaces. This value of 19 kcal/mole is identical to that obtained independently from the parameters in the standard L–H rate expression (Table 5) and is a further indication of the self-consistency of these parameters.

SUMMARY

The catalytic behavior of Pd/δ-Al_2O_3 catalysts was thoroughly determined over a range of temperature and O_2 pressure that has been infrequently studied. Infrared spectra were simultaneously obtained under different steady-state reaction conditions to monitor the CO species present on the Pd surface. As the temperature increased, the

apparent activation energy increased, the pressure dependency on CO changed from near zero order to negative first order, and the O_2 dependency increased from 0.2 to 0.7 at pressures above 50 Torr. At temperatures below 400 K, a region of first-order O_2 dependence was also observed at lower O_2 pressures. The IR spectra were consistent with the negative-order dependence on CO, and higher rates were observed when the surface concentration of CO decreased. These spectra also provided evidence that compressed layers of CO existed below 400 K at the relative high O_2 pressures employed in this study.

By comparing these IR results with those from previous studies, a normal Langmuir–Hinshelwood model appears applicable in the regime above 400 K, whereas a reaction between CO and O atoms at the perimeters of their respective islands seems more appropriate at higher O_2 pressures in the regime below 400 K. Computer fitting the rate equations derived from each model to both regimes indeed showed that each fits its respective region better over these limited ranges of temperature and pressure, and the rate parameters derived from each equation were consistent with this transformation. The true activation energy of the rds shifted from 15 kcal/mole in the island regime to 23 kcal/mole in the normal L–H regime. This agrees with the shift from 14 to 25 kcal/mole reported by Engel and Ertl from their molecular beam investigation of this reaction on a Pd(111) surface (*3*). Furthermore, the heats of adsorption derived from the K_{CO} and K_{O_2} values in the L–H rate expression were quite similar to Q_{ad} values measured on nearly saturated Pd surfaces, and the shift in each parameter to a lower value in the island rate expression is expected as the compression in each island would weaken bond strengths. Finally, a partial analysis of the kinetic behavior in the regime of first-order O_2 dependency, where O_2 adsorption is the slow step, indicates that the activation energy for O_2 adsorption remains zero or near zero on these CO-covered Pd surfaces at these reaction conditions.

ACKNOWLEDGMENTS

This study was sponsored by a grant from Teledyne Water Pik, Fort Collins, CO. Additional support was provided by the Mobil Research and Development Corporation, Princeton, NJ.

REFERENCES

1. Langmuir, I., *Trans. Faraday Soc.* **17,** 672 (1922).
2. Engel, T., and Ertl, G., *in* "Advances in Catalysis" (D. D. Eley, H. Pines, and P. B. Weisz, Eds.), Vol. 28, p. 1. Academic Press, New York, 1979.
3. Engel, T., and Ertl, G., *J. Chem. Phys.* **69,** 1267 (1978).
4. Boudart, M., and Djéga-Mariadassou, "Kinetics of Heterogeneous Catalytic Reactions," p. 105. Princeton Univ. Press, Princeton, NJ, 1984.
5. Cant, N. W., Hicks, P. C., and Lennon, B. S., *J. Catal.* **54,** 372 (1978).
6. Ladas, S., Poppa, H., and Boudart, M., *Surf. Sci.* **102,** 151 (1981).
7. Berlowitz, P. J., Peden, H. F., and Goodman, D. W., *J. Phys. Chem.* **92,** 5213 (1988).
8. Weinberg, W. H., Comrie, C. M., and Lambert, R. M., *J. Catal.* **41,** 493 (1976).
9. Mantolin, B., and Gillet, E., *Surf. Sci.* **166,** L115 (1986).
10. Gillet, E., Channakhone, S., and Mantolin, V., *Surf. Sci.* **152,** 603 (1985).
11. Rumpf, F., Poppa, H., and Boudart, M., *Langmuir* **4,** 723 (1988).
12. Stuve, E. M., Madix, R. J., and Brundle, C. R., *Surf. Sci.* **146,** 155 (1984).
13. Conrad, H., Ertl, G., and Küpper, S. J., *Surf. Sci.* **76,** 323 (1978).
14. Mukesch, D., Morton, W., Kenney, C. N., and Cutlip, M. B., *Surf. Sci.* **138,** 237 (1984).
15. Lynch, D. T., and Wanke, S. E., *J. Catal.* **88,** 333 (1984).
16. Kaul, D. J., and Wolf, E. E., *J. Catal.* **93,** 321 (1985).
17. Ehsasi, M., Seidel, C., Ruppender, H., Draschel, W., Block, J., and Christman, K., *Surf. Sci.* **210,** 6198 (1989).
18. Keverekidis, I., Schmidt, L. D., and Aris, R., *Surf. Sci.* **137,** 151 (1984).
19. Baddour, R. F., Modell, M., and Heusser, U. K., *J. Phys. Chem.* **72,** 3621 (1968).
20. Kember, D. R., and Sheppard, N., *J. Chem. Soc. Faraday Trans.* **77,** 1309 (1981).
21. Choi, K. I., and Vannice, M. A., *J. Catal.* **127,** 465 (1991).
22. Choi, K. I., and Vannice, M. A., *J. Catal.* **127,** 489 (1991).
23. Choi, K. I., and Vannice, M. A., *J. Catal.*, **131,** 22 (1991).

24. Choi, K. I., and Vannice, M. A., *J. Catal.* **131,** 36 (1991).
25. Palmer, M. B., and Vannice, M. A., *J. Chem. Technol. Biotechnol.* **30,** 205 (1986).
26. Chou, P., and Vannice, M. A., *J. Catal.* **104,** 17 (1987).
27. Chou, P., and Vannice, M. A., *J. Catal.* **105,** 342 (1987).
28. Bradshaw, A. M., and Hoffmann, F., *Surf. Sci.* **72,** 513 (1978).
29. Conrad, H., Ertl, G., Koch, J., and Latta, E. E., *Surf. Sci.* **41,** 462 (1974).
30. Baddour, R. F., Modell, M., and Goldsmith, R. L., *J. Phys. Chem.* **74,** 1787 (1970).
31. Eischens, R. P., Francis, S. A., and Plisken, W. A., *J. Phys. Chem.* **60,** 794 (1956).
32. Eischens, R. P., and Plisken, W. A., *in* "Advances in Catalysis" (D. D. Eley, W. G. Frankenburg, and V. I. Komarewsky, Eds.), Vol. 10, p. 1. Academic Press, New York, 1958.
33. Palazov, A., Chang, C. C., and Kokes, R. J., *J. Catal.* **36,** 338 (1975).
34. Garland, C. W., Lord, R. C., and Triano, P. F., *J. Phys. Chem.* **69,** 1188 (1965).
35. Sheppard, N., and Nguyen, T. T., *Adv. Infrared Raman Spectrosc.* **5,** 67 (1978).
36. Vannice, M. A., Wang, S.-Y., and Moon, S. H., *J. Catal.* **71,** 152 (1981).
37. Boecker, D., and Wicke, E., *Ber. Bunsenges. Phys. Chem.* **89,** 629 (1985).
38. Li, Y.-E., Boecker, D., and Gonzalez, R. D., *J. Catal.* **110,** 319 (1988).
39. Ichikawa, S., Poppa, H., and Boudart, M., *in* "ACS Advances in Chem. Series" (T. E. Whyte *et al.*, Eds.), p. 439. Am. Chem. Soc., Washington, DC, 1984.
40. Boudart, M., and Rumpf, F., *React. Kinet. Catal. Lett.* **35,** 95 (1987).
41. Razon, L. F., and Schmitz, R. A., *Catal. Rev.-Sci. Eng.* **28,** 89 (1986).
42. Ladas, S., Imbihl, R., and Ertl, G., *Surf. Sci.* **198,** 42 (1988).
43. Schuth, F., and Wicke, E., *Ber. Bunsenges. Phys. Chem.* **93,** 491 (1989).
44. Turner, J. E., and Maple, M. B., *Surf. Sci.* **147,** 647 (1984).
45. Sales, B. C., Turner, J. E., and Maple, M. B., *Surf. Sci.* **114,** 381 (1982).
46. Plath, P. S., Moller, K., and Jaeger, N. I., *J. Chem. Soc. Faraday Trans.* **84,** 1751 (1988).
47. Luss, D., "Chemical Reactor Theory—A Review." Prentice-Hall, Englewood Cliffs, NJ, 1977.
48. Burrows, V. A., Sundaresan, S., Chabal, T. J., and Christman, S. B., *Surf. Sci.* **180,** 110 (1987).
49. Collins, N. A., Sundaresan, S., and Chabal, T. J., *Surf. Sci.* **180,** 136 (1987).
50. Matsushima, T., and White, T. M., *J. Catal.* **39,** 265 (1975).
51. Matsushima, T., Almy, D. B., Foyt, D. C., Close, J. S., and White, T. M., *J. Catal.* **39,** 277 (1975).
52. Matsushima, T., and White, T. M., *J. Catal.* **40,** 334 (1975).
53. Matsushima, T., Mussett, C. J., and White, T. M., *J. Catal.* **41,** 397 (1976).
54. Matsushima, T., and White, T. M., *Surf. Sci.* **67,** 122 (1977).
55. Poppa, H., and Soria, F., *Surf. Sci.* **115,** L105 (1982).
56. Barshad, Y., and Gulari, E., *J. Catal.* **94,** 468 (1985).
57. Vorontsov, A. V., Kasatkina, L. A., Dzisyak, A. P., and Tikhonova, S. V., *Kinet. Katal.* **20,** 1194 (1979).
58. Voronstov, A. V., and Kasatkina, L. A., *Kinet. Katal.* **21,** 1494 (1980).
59. Engel, T., *J. Chem. Phys.* **69,** 373 (1978).
60. Yao, Y. Y-F., *J. Catal.* **87,** 152 (1984).
61. Schwab, G. M., and Gossner, K., *Z. Phys. Chem. Neue Folge* **16,** 39 (1958).
62. Tajbl, D. G., Simmons, J. B., and Carberry, J. J., *Ind. Eng. Chem.* **5,** 171 (1966).
63. Sass, A. S., Shvets, V. A., Savel'eva, G. A., Popova, N. M., and Kazanski, V. B., *Kinet. Katal.* **27,** 894 (1986).
64. Papp, H., and Kamp, P., *Surf. Interface Anal.* **12,** 253 (1988).
65. Bond, G. C., Fuller, M. J., and Molloy, L. R., *in* "Proceedings, 6th International Congress on Catalysis, London, 1976" (G. C. Bond, P. B. Wells, and F. C. Tompkins, Eds.), Vol. 1, p. 356. The Chemical Society, London, 1977.
66. Stark, O. S., and Harris, M. R., *J. Phys. E. Sci. Instrum.* **16,** 492 (1983).
67. Inoue, Y., Yoshioka, I., and Sato, K., *J. Phys. Chem.* **88,** 1148 (1984).
68. Landry, S. M., Dalla Betta, R. A., Lu, J. P., and Boudart, M., *J. Phys. Chem.* **94,** 1203 (1990).
69. Matsushima, T., and Asada, H., *J. Chem. Phys.* **85,** 1658 (1986).
70. Zhou, X., and Gulari, E., *Langmuir* **2,** 709 (1986).
71. Mishchenko, Yu. A., Kakhniashvili, G. N., Marshakova, E. N., Dulin, D. A., and Geĭbshtein, A. I., *Kinet. Catal.* **28,** 538 (1987).
72. Szilagyi, T., Sarkany, A., Mink, J., and Tetenyi, P., *Acta. Chim. Acad. Sci. Hungar.* **100,** 1109 (1979).
73. Ertl, G., and Korch, J., *Z. Naturforsch* **259,** 1960 (1970).
74. Tracy, J. C., and Palmberg, P. W., *J. Chem. Phys.* **51,** 4852 (1969).
75. Behm, R. J., Christmann, K., and Ertl, G., *J. Chem. Phys.* **73,** 2984 (1980).
76. Conrad, H., Ertl, G., Kuppers, J., and Latta, E. E., *Surf. Sci.* **65,** 245 (1977).
77. Ertl, G., and Koch, J., *J. Phys. Chem. N.F.* **69,** 323 (1970).

78. Ertl, G., and Rau, P., *Surf. Sci.* **15,** 443 (1969).
79. Bortner, M. H., and Parravano, G., *in* "Advances in Catalysis" (D. D. Eley, W. G. Frankenburg, and V. I. Komarewsky, Eds.), Vol. 9, p. 424 Academic Press, New York, 1957.
80. Brennan, D., Hayward, D. O., and Trapnell, B. M. W., *Proc. R. Soc. A* **256,** 81 (1960).
81. Ertl, G., and Koch, J., *in* "Proceedings, 5th International Congress on Catalysis, Palm Beach, 1972" (J. W. Hightower, Ed.), p. 969, North-Holland, Amsterdam, 1973.
82. Zakumbaeva, G. D., Zakarina, N. A., Naidin, V. A., Dostiyarov, A. M., Toktabaeya, N. F., and Litvyakova, E. N., *Kinet. Catal.* **24,** 379 (1983).
83. Boudart, M., Mears, D. E., and Vannice, M. A., *Ind. Chem. Belge* **32,** 281 (1967).